CLINICAL ORTHOPAEDICS AND RELATED RESEARCH
Number 336, pp 297–307

Cement Debonding Process of Total Hip Arthroplasty Stems

N. Verdonschot, PhD; and R. Huiskes, PhD

Retrieval studies have indicated that debonding of the stem cement interface in total hip arthroplasty precedes clinical failure of femoral components. This study addressed the mechanisms that play a role in the debonding process by analyzing how debonding is likely to proceed in the course of time. It was investigated whether debonding is an immediate process or if it is likely to develop slowly with time, which interface stress components contribute particularly to its progression, and whether the mechanical integrity of the cement mantle is likely to be compromised by the debonding process. To answer these questions, a 3-dimensional finite element model of a femoral total hip arthroplasty reconstruction was developed and used to simulate the debonding process. The results showed that debonding was governed by the shear stress component at the interface. Debonding started in the tip region and the proximal, medial anterior region. These debonded regions expanded until the whole interface was de bonded. Cement stresses slowly increased at the end of the debonding process to a level twice as high as the initial one. The probability of debonding, as measured by an interface failure index, remained constant as debonding progressed. This indicates that, for this particular design, much less surface area is required for load transfer than is provided by the stem, and the debonding process does not necessarily accelerate quickly once debonding is initiated.

Cemented total hip arthroplasty is 1 of the most successful operations worldwide. However, an increasing number of revisions are needed every year. Factors affecting the revision rate are difficult to delineate.[14] Loosening of the femoral component often is accompanied by cement fractures and disruption of the stem cement interface. In retrieved specimens it was found by Jasty et al[17] that cement fractures and disruption of the stem cement interface are apparent long before clinical failure of the reconstruction occurs. These authors suggested that cement failure was preceded by local loosening of the stem-cement interface. Thus, it seems to be of clinical importance to obtain a firm and lasting bond between stem and cement.[15]

A number of authors have reported the strength of the stem cement bond. Using polymethylmethacrylate uncoated and precoated specimens, Raab et al[22] investigated the static and fatigue performance of the stem cement interface. They found static shear strengths of 6.9 to 12.5 MPa for dry tested specimens. However, after immersing the specimens in

From Biomechanics Section, Institute of Orthopaedics, University of Nijmegen, Nijmegen, The Netherlands.

Reprint requests to Rik Huiskes, PhD, Biomechanics Section, Institute of Orthopaedics, University of Nijmegen, PO Box 9101, 6500 HB Nijmegen, The Netherlands.

Received: October 18, 1995.

Revised: March 11, 1996.

Accepted: June 18, 1996.

saline, shear strengths dropped to 5.3 to 6.7 MPa. The fracture toughness of the stem cement interface appeared to be only 17% of that of bone cement. Barb et al[2] determined the shear strength of the stem cement interface after several periods of implantation in dogs. They found average strengths of 4.8 to 8.4 MPa; the strengths decreased during the implantation period. Stone et al[26] showed significant reductions in shear strengths when the bone cement or the stem surface was contaminated during total hip arthroplasty. Arroyo and Stark[1] investigated the effect of surface roughness on the shear strength of the stem cement interface. An increase in strength from 0.8 to 10 MPa was found with increasing roughness from 1.6 to 7.7 μm. Experiments to test the tensile strength of the stem cement interface have been reported by Keller et al.[18] They found bonding strengths between 5.4 and 11.0 MPa when specimens were made during the doughy phase of cement. Although these data illustrate the static strength of the stem cement bond and the factors that are of importance, it is more appropriate to test the interface dynamically in fatigue tests. However, because of the duration of these tests and the large number of parameters involved, few data on this subject are published. Using a cantilever rotating bending test, Raab et al[22] measured the fatigue strengths of the stem cement interface and found a range of 1 to 3 MPa after 5×10^6 loading cycles. Davies et al[7] performed a fatigue pushout test with sinusoidal stress levels ranging from 0 to 1.25 MPa. The interface failed after approximately 10,000 loading cycles.

Comparing the static and fatigue strength data with the stresses expected, which can be as high as 8 MPa,[10,13,20,23,27] suggests that it is likely that the stem cement interface will (partly) fail. If the failure does not occur in the immediate postoperative period, it almost certainly will occur after long term, dynamic loading. In fact, after having analyzed a large amount of retrieved material, Harris[11] came to the following conclusion: "The mechanism of failure of loosening of cemented femoral components is now known. It is debonding at the cement metal interface."

This study addressed the mechanisms that play a role in the debonding process. Whereas most prior clinical and experimental investigations considered the behavior of the reconstruction for a bonded versus a debonded stem cement interface, the authors studied how debonding is likely to proceed in the course of time. Questions asked were whether debonding is an immediate process or if it is likely to develop slowly with time, which interface stress components contribute particularly to its progression, if full or partial coating patches or roughness patterns could potentially arrest its progress, and whether the mechanical integrity of the cement mantle is likely to be compromised by the debonding process. To answer these questions, a 3-dimensional finite element model of the femoral total hip arthroplasty reconstructions was developed and used to simulate the debonding process.

MATERIALS AND METHODS

An embalmed femur was scanned using computed tomographic techniques in slices of 4-mm thickness, perpendicular to the femoral axis at 27 locations. Using a computer graphics program, a finite element model of the bone was made, based on the contours and densities of the computed tomography (CT) data. Subsequently, a finite element model of a hip prosthesis was created and introduced in the bone model. In the proximal medial region, the cement mantle had a minimal thickness of 4 mm. In the other regions, the cement mantle had a thickness of at least 2 mm. Directly distal to the tip no cement was present, simulating a void created by a centralizer. The model contained 2130 8-node isoparametric elements and 3360 nodal points.

For each bone element the average apparent density $\rho(gr/cm^3)$ was determined using the CT data. From these values, Young's moduli (MPa) could be calculated for each individual bone element using[4]

$$E = c\,\rho^3; \qquad (1)$$

with $c = 3790\ (MPa/(gr/cm^3))^3$.

For the bone elements, Poisson's ratio was chosen as 0.35. Figure 1 illustrates the density distribution in the bone. Young's modulus for the cement material was set at 2.2 GPa, and Poisson's ratio at 0.3. The prosthesis was assumed to be made out of stainless steel with an elastic modulus of 200 GPa and a Poisson's ratio of 0.28.

One loading case, representing the stance phase of gait, was considered (Fig 1). This load was assumed to be applied repeatedly. The force applied to the prosthetic head was 2450 N, with angles at 23° in the frontal plane and 6° in the sagittal plane.[3] Three muscle forces (gluteus minimus, medius, and maximus) were included that acted on the greater trochanter. The magnitudes of these forces were estimated from Crowninshield and Brand.[5] The directions of the muscle forces were determined using the flexion angle and the points of attachment of the muscles, as described by Dostal and Andrews.[8] The resultant muscle force was 1650 N, with angles at 24° in the frontal plane and 15° (directed toward anterior) in the sagittal plane.

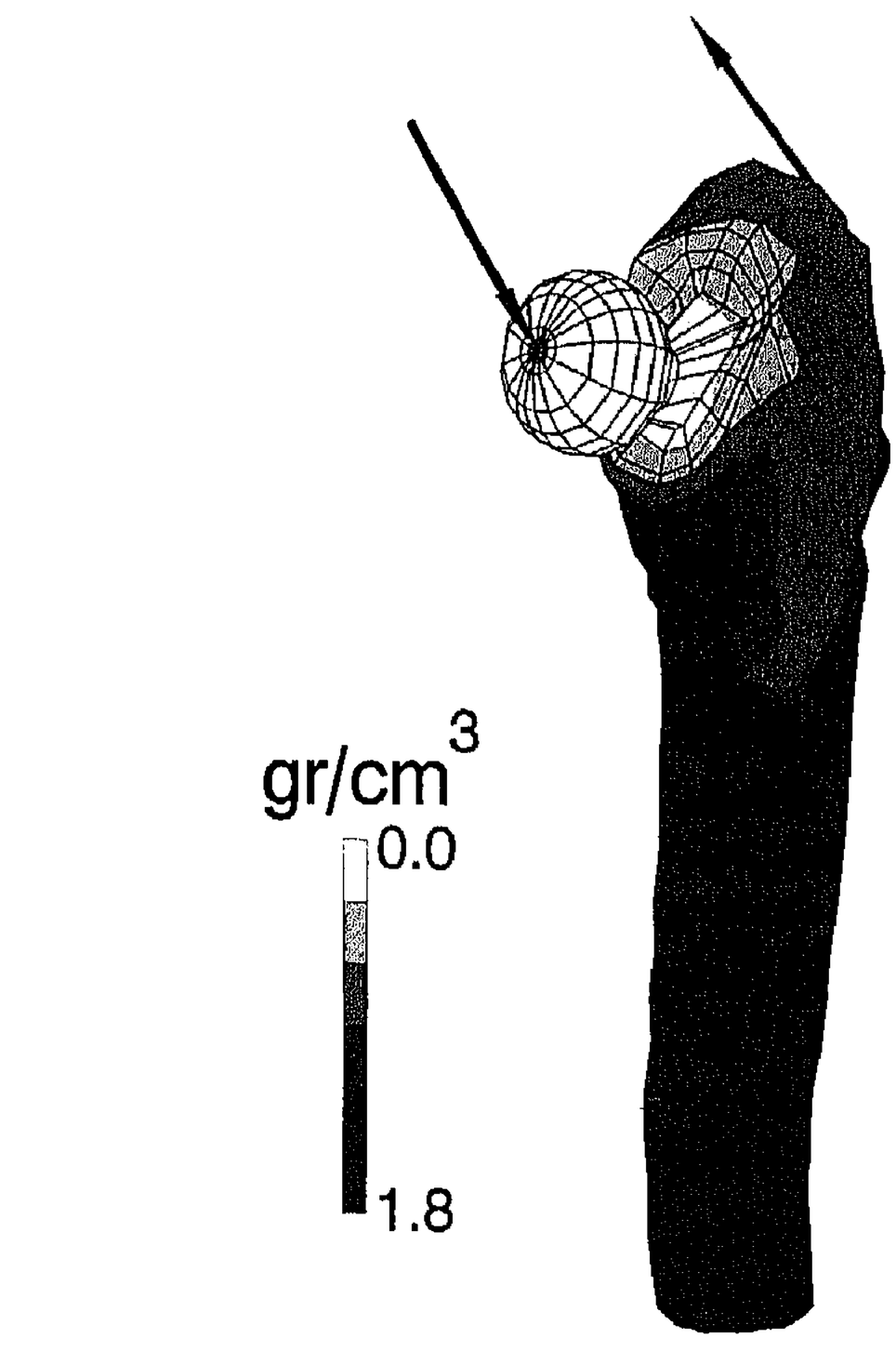

Fig 1. The finite element model of the prosthesis cement bone structure (posterior medial view). Bone density distribution is indicated on a gray scale. The hip joint force and 3 muscle forces were assumed to represent the stance phase of gait loading conditions.

To be able to simulate the debonding process, 281 gap elements were situated at the stem cement interface (Marc Analysis Corporation, Palo Alto, CA). At debonded sites, a friction coefficient of 0.25 was assumed.[21] To investigate the effects of reduced friction provided by soft tissue interposition, the extreme case of no friction also was considered in the analyses.

Initially, the gap elements were deactivated, and the stem cement interface was assumed fully bonded. At locations where the interface became unbonded, the bond between stem and cement was removed, and gap elements were activated. To determine where local debonding would occur, a multiaxial Hoffman's failure index[12] was used. Hoffman used this index to determine material failure exposed to a multiaxial stress situation. The same procedure was successfully applied by Stone et al[25] to establish failure of cancellous bone. Weinans et al[28] incorporated this index in a finite element model simulating the process of prosthesis bone disruption. The Failure Index (*FI*) is defined as

$$FI = \frac{1}{S_t}\frac{1}{S_c}\sigma^2 + \left(\frac{1}{S_t} - \frac{1}{S_c}\right)\sigma + \frac{1}{S_s^2}\tau^2 \quad \text{where bonded,} \qquad (2/a)$$

and

$$FI = 0 \text{ where debonded,} \qquad (2/b)$$

where $S_t = 8$ MPa is the tensile strength of the interface,[18] $S_c = 70$ MPa is the compressive strength of the interface (the compressive strength of acrylic cement according to Saha and Pal[24]), $S_s = 6$ MPa is the shear strength of the interface,[1,2,22,26] and σ is the normal and τ is the shear stress at the interface. For a particular value of the shear stress, the failure index is higher for tensile stresses than for compressive ones. Thus, a combination of shear and tension is assumed to be more harmful to the interfacial bond than is shear in combination with compression.

In the analyses, it was assumed that complete interface debonding eventually occurred. Thus, the failure index was not used to determine if interface failure would occur, but to identify where along the interface this would happen. The debonding process was simulated iteratively in this study. The iteration scheme is illustrated in

Figure 2. In the simulation, the values of failure index at every interfacial nodal point were calculated. At the location where the failure index was maximal, the interface was debonded and a gap element was activated. Because of this change in local interface condition, new stress patterns were obtained, and a new finite element calculation was necessary. In the next increment, the maximal failure index was calculated again, and a new location for interface disruption was determined. In this way, the process of gradual debonding of the prosthesis was simulated without consideration of the actual time axis of the debonding process. Stress levels in the cement and at the interfaces were assessed as debonding of the interface progressed.

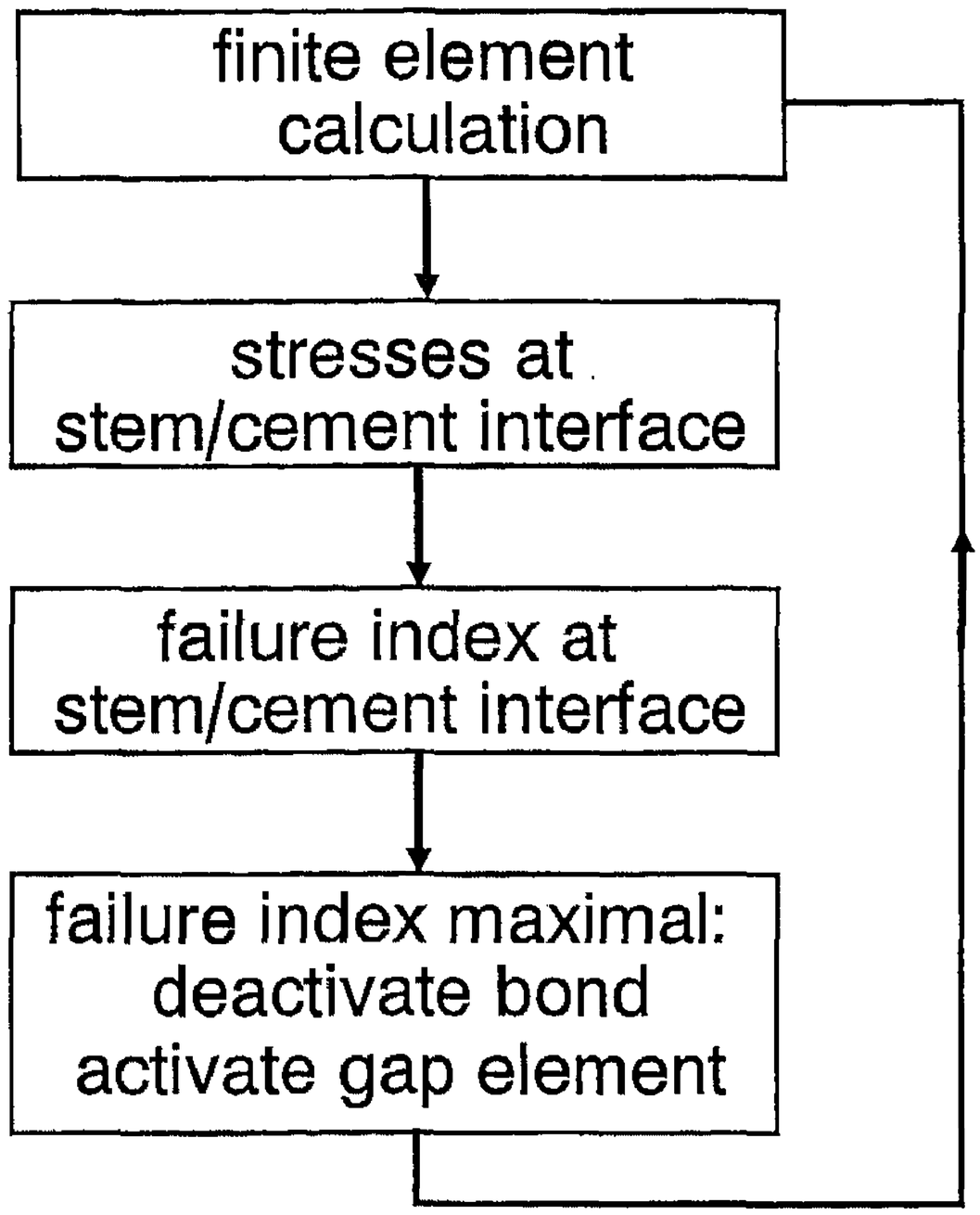

Fig 2. The iterative simulation scheme of the debonding process. First, the stresses at the stem cement interface are calculated. Next, the values for the failure indexes are calculated. The interface is debonded where this value is maximal, and a new finite element calculation follows.

RESULTS

Initially, high interface stresses were generated at the proximal and distal regions. These were the first to debond. Debonding started in the tip region but was directly followed by debonding in the proximal, medial-anterior region. These debonded sites expanded until the whole interface was loose. The proximal lateral region was the last to debond. Figure 3 illustrates this by showing the state of debonding after ensuing percentages of total debonded area. In the case that idealized frictionless conditions were assumed at the debonded areas ($\mu = 0.0$), the debonding process developed in a virtually identical sequence.

The evolution of the debonding process was governed by high interface stresses generated directly around the debonded areas. Specifically, the shear stress patterns seemed to outline the debonded stem cement interface areas (Fig 4). This resulted in high values for the failure index and subsequent debonding of these regions. The maximal shear and tensile stress values generated at the stem cement interface showed irregular patterns as debonding proceeded, depending on the local interface situation. However, maximal compressive stresses increased gradually with the amount of debonded area. Initially, the maximal compressive stress was 3.8 MPa, which increased to a value of 10.4 MPa after complete debonding. Assuming idealized frictionless stem cement interface conditions at debonded sites, the compressive interface stresses increased considerably more after complete debonding, to a maximal value of almost 36 MPa.

The debonding process had only moderate effects on the overall stress patterns in the cement mantle. High cement stresses were found in the tip region and at the medial proximal side throughout the debonding process (Fig 5). In debonded areas as great as 50%, the stress intensity in the cement mantle hardly changed. When 75% of the interface area was debonded, an increase in stress intensity was found in the cement mantle. Complete debonding of the stem changed the load transfer mechanism and produced tensile stress levels that were twice as high as the initial ones. The stresses generated in the cement were

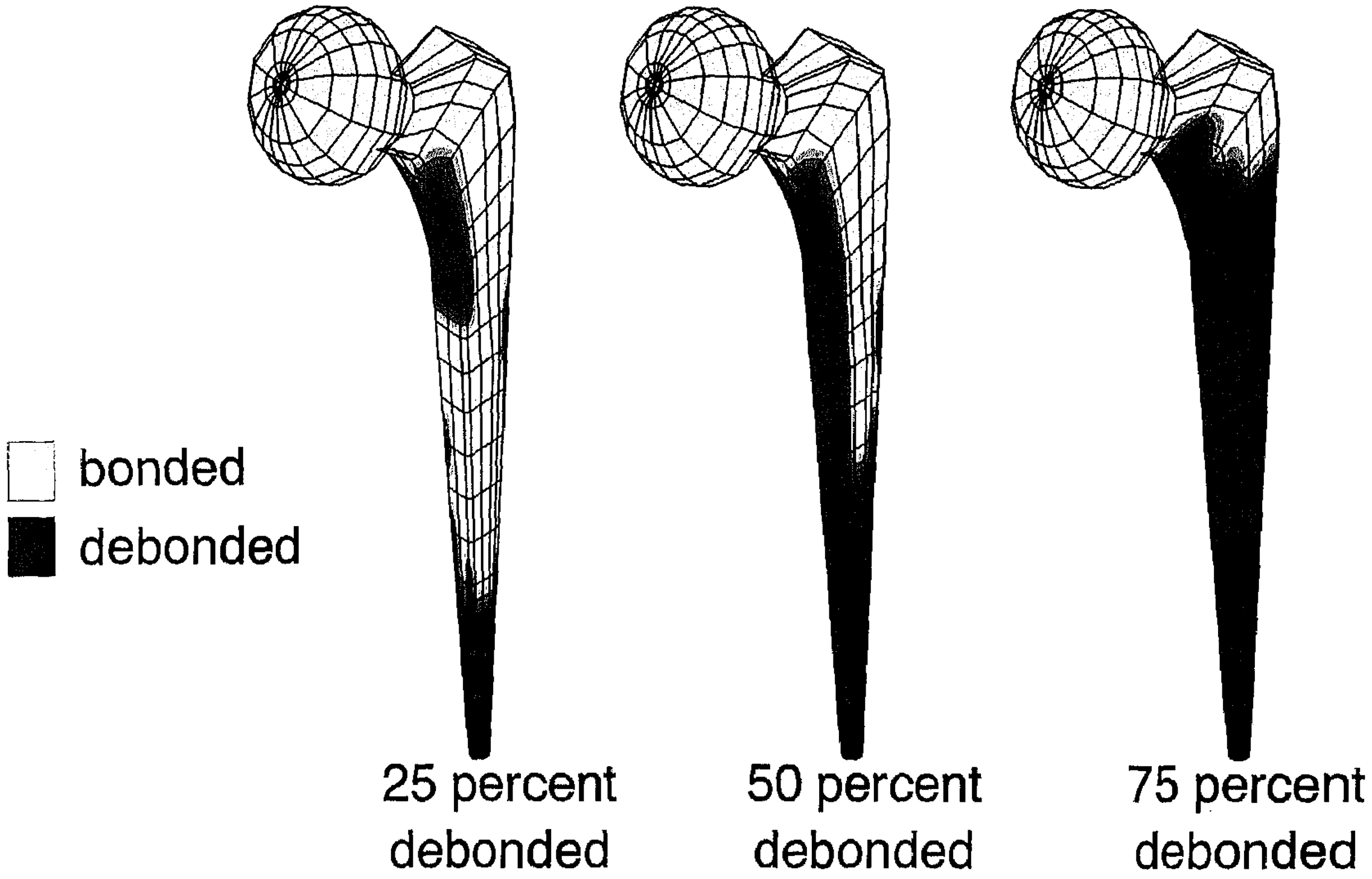

Fig 3. The debonded sites at various stages in the debonding process. Debonding started at the distal and proximal side. These debonded sites expanded until the whole interface was loose.

governed not only by the global load transfer mechanism, but also by the local stem cement interface conditions. Around the edges of the debonded areas, high shear stresses were apparent where bonding still existed. These concentrations of load transfer at these sites also caused high local cement stresses in these regions (Fig 6). While the debonded area expanded further along the interface, the shear stresses were released, and with them, the local cement stresses. The maximal tensile stress in the cement mantle slowly increased as debonding of the stem cement interface proceeded (Fig 7). Maximal stress peaks were 2.6 and 5.7 MPa before and after debonding, respectively. Assuming an idealized, frictionless stem cement interface, a maximal cement stress peak was generated of almost 17 MPa after the interface had completely debonded. The increase of cement stress in this case was predominantly obtained in the last part of the debonding process (Fig 7).

The debonding process was remarkably stable, indicating that much less surface area is required for load transfer than is provided by the stem. Starting with a fully bonded stem, the maximal failure index was approximately 0.4 and was generated at the tip of the prosthesis (Fig 8). This indicates that no direct failure would be expected immediately after surgery. Assuming a decreasing interface strength with the number of loading cycles, this was the first prosthetic point that was debonded from the cement mantle. After this point had debonded, the maximal value of the failure index (occurring also in the tip region) increased to a value of more than 1.0, indicating rapid debonding at that stage. Subsequently, the maximal value of the failure index decreased again and remained at a rather constant level as loosening progressed, varying between 0.1 and 0.3. As the bonded area is reduced, one could expect that the interface stresses would increase, thereby elevating the

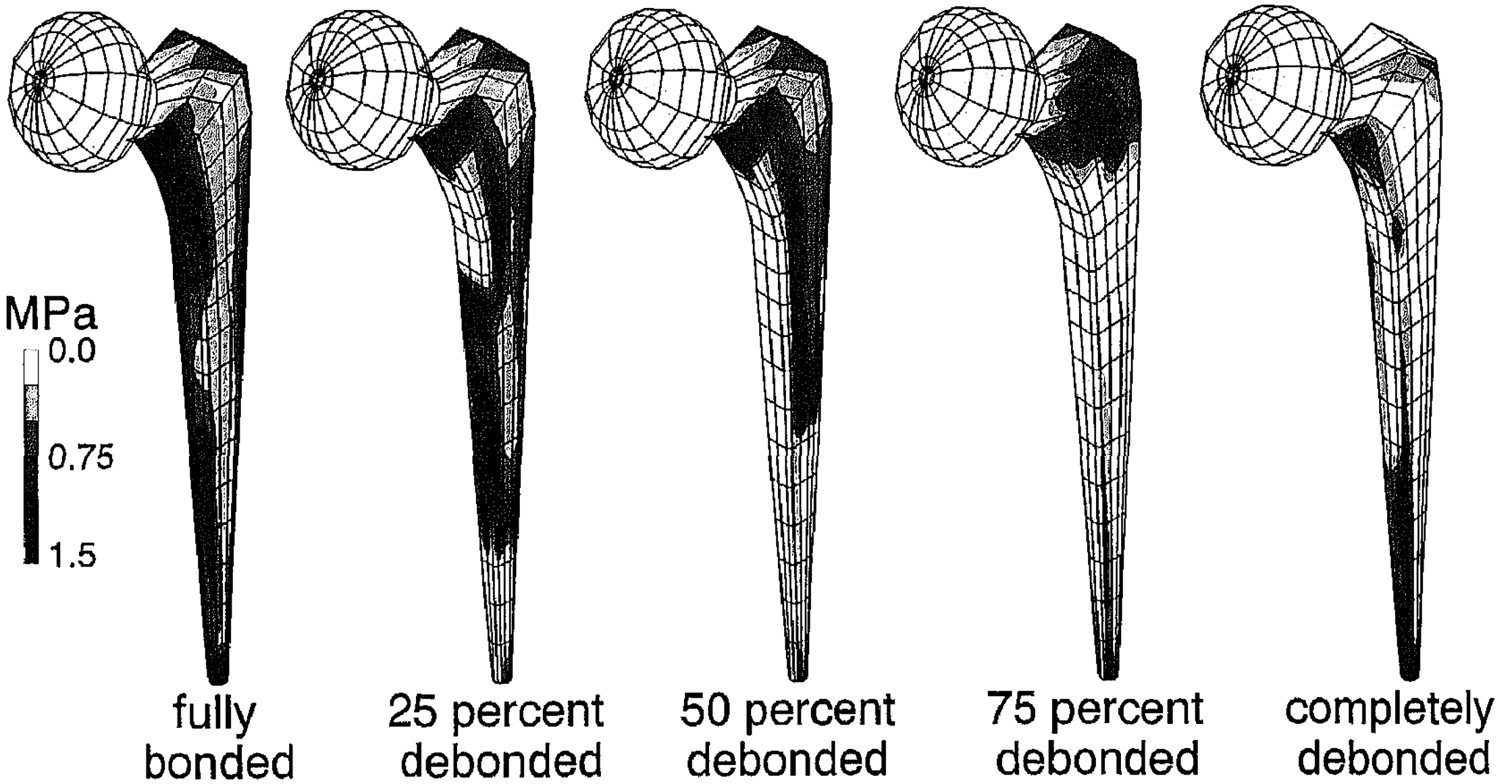

Fig 4. The shear stress patterns at the stem cement interface at various stages in the debonding process. The shear stress patterns seemed to outline the debonded areas and governed the debonding process.

failure index in the bonded areas. As can be seen in Figure 8, this was hardly the case. Even after the prosthesis was almost completely debonded, the maximal failure index did not increase substantially. Thus, the probability of interface debonding hardly increases during the debonding process. This indicates that the area available for load transfer provided by the stem is larger than needed and that the initiation of debonding does not necessarily lead to an acceleration of the debonding process. Assuming idealized frictionless stem cement interface conditions at debonded sites, a different pattern of the failure index was found as debonding progressed (Fig 8). In that case, debonding of the last 15% of interface surface increased the failure index, indicating unstable, rapid debonding of the stem cement interface in that stage.

Although, the value of the failure index is determined by the values of the normal and shear stress components, it was the latter that governed the debonding process. Compressive and tensile stresses (maximally 8 and 1.5 MPa, respectively) were much smaller than the static strengths (70 and 8 MPa, respectively), whereas the shear stress component reached values close to the strength of 6 MPa (Fig 9).

DISCUSSION

It must be appreciated that the method used in this study has a number of limitations. Only 1 particular stem shape was considered. Different stem shapes are known to generate different interface stress patterns.[13] Thus, shape affects the evolution of the debonding process. The stem was assumed to be initially fully bonded to an intact cement mantle. The mechanical properties of the acrylic cement were assumed to remain constant during the debonding process, so no cement failure or creep of the cement material was simulated. Bone geometry and density distribution were based on CT data of 1 average bone. The mechanical bone properties were assumed to be isotropic and to remain constant in time, whereas in reality, bone is anisotropic and is subject to continuous remodeling. The con-

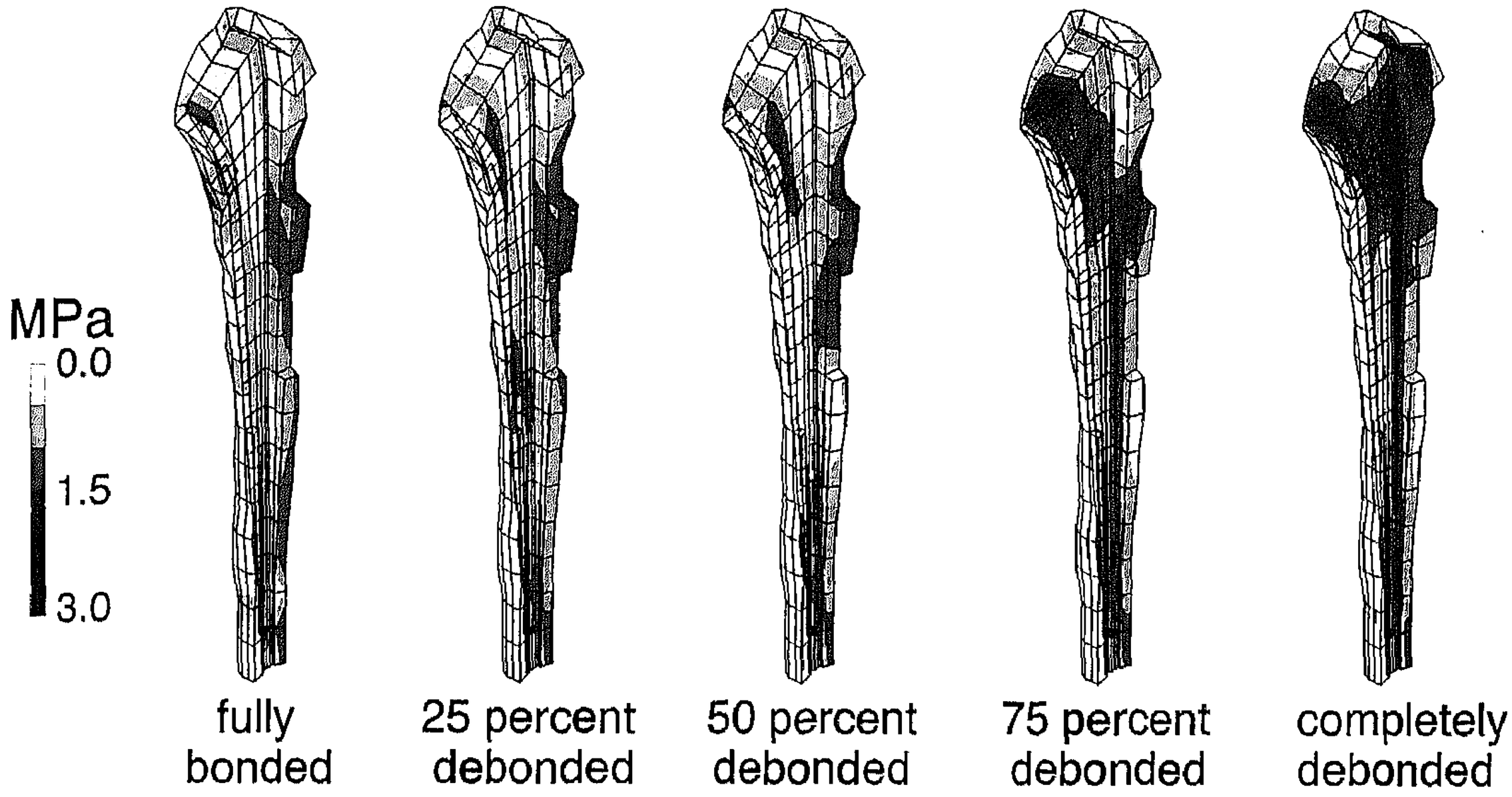

Fig 5. The tensile stress distribution in the cement mantle at various stages in the debonding process. Stress levels remained virtually unaffected until more than 50% of the interface area had debonded.

stants in the failure index are based on experiments that considered only 1 stress component at the interface. Thus, the effect of combined stresses at the interface, as accounted for in the definition of the failure index, was estimated but not actually verified.

Debonding also can be analyzed using the theory of fracture mechanics. This theory assumes a stress intensity at the crack tip that governs the crack initiation and propagation. Similar to the method used in this study, the theory considers failure attributable to normal stresses (Mode I) and shear stresses (Mode II). However, this method can not be used yet because there are no experimental data available that include the mixed loading modes of shear and normal (tensile and compression) stresses at the interface in relation

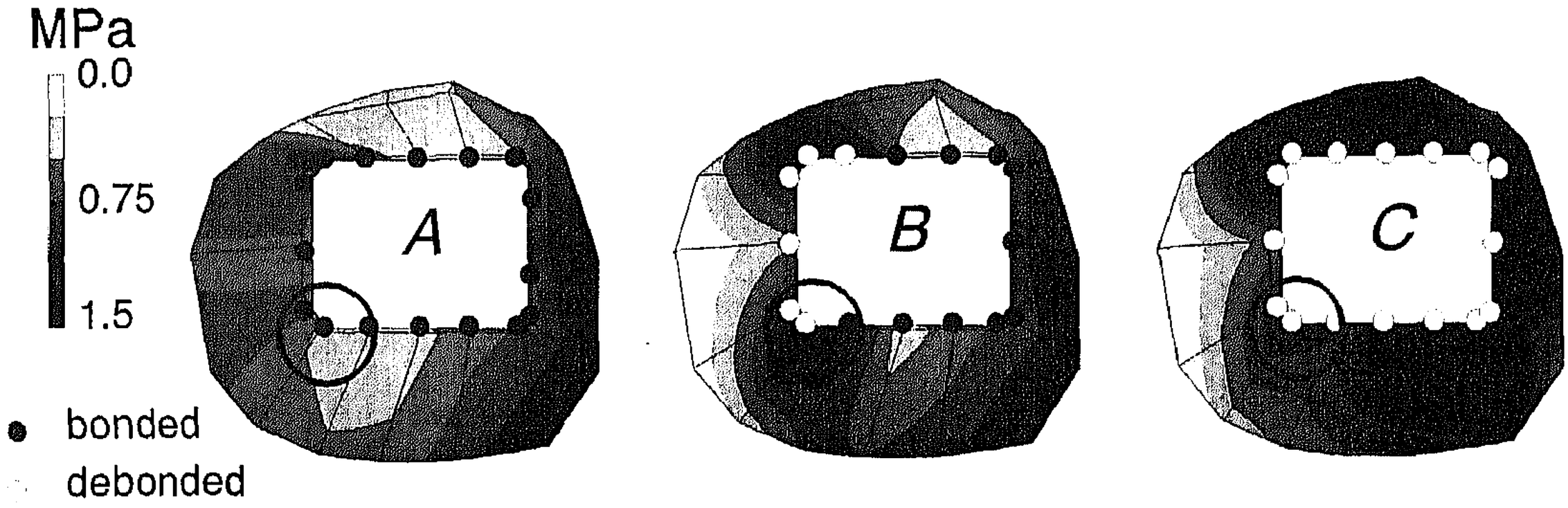

Fig 6A–C. The tensile stress distribution in the cement mantle in a transverse cross section, 4 cm below the resection level. Interface conditions are (A) fully bonded, (B) partially debonded, and (C) completely debonded. Around the edges of the debonded areas, concentrations of load transfer sometimes induced high local cement stresses in these regions (encircled), which were released again when the debonded area expanded further along the interface.

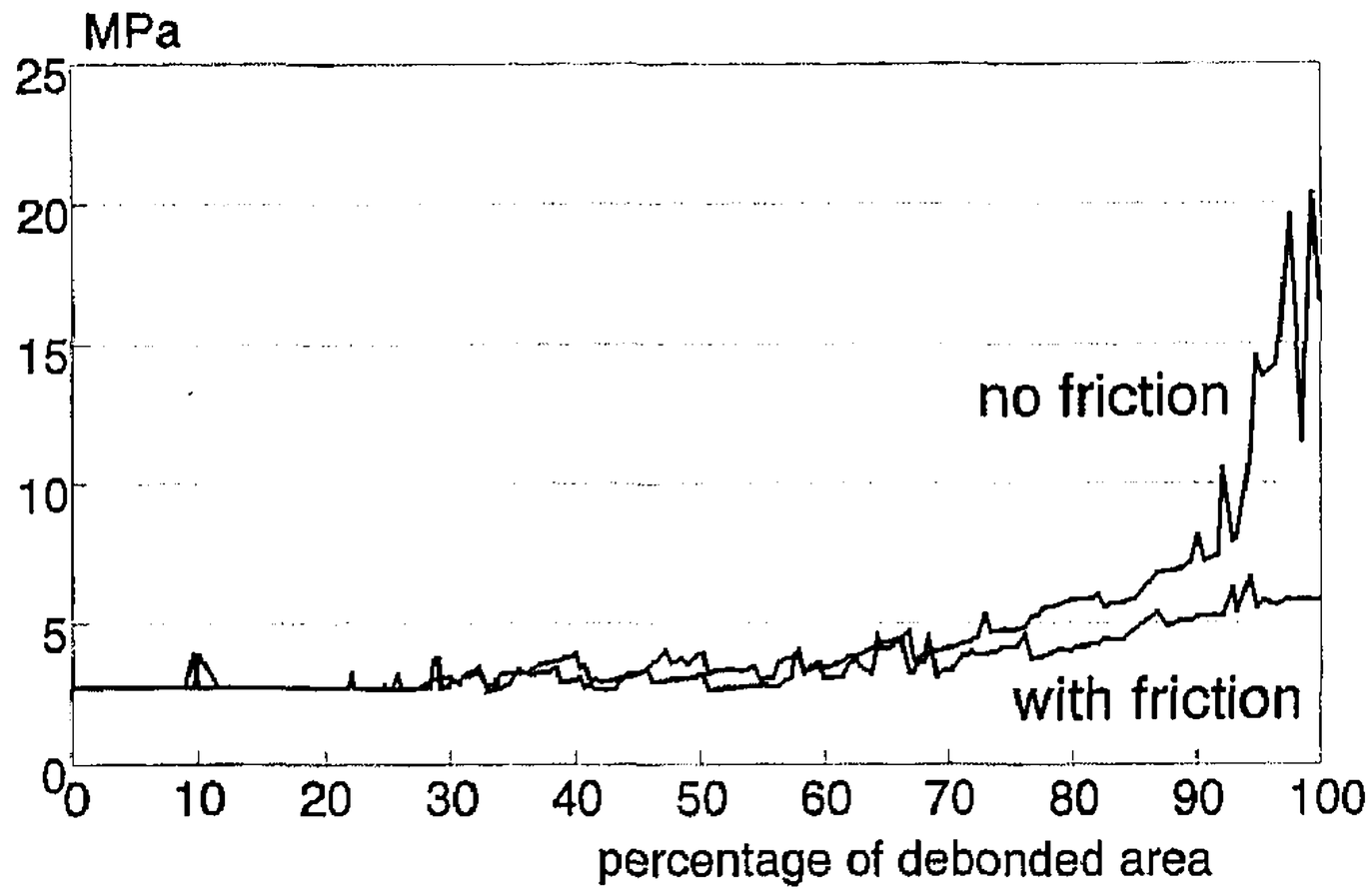

Fig 7. The development of the maximal tensile stress generated in the cement mantle during the debonding process. After 50% of the interface area had debonded, the maximal tensile stress gradually increased. Assuming frictionless stem cement interface conditions at the debonded sites, resulted in higher cement stresses during the last part of the debonding process.

to initiation and propagation of stem cement debonding. The time scale that would indicate how long the loosening process would take was not determined because not enough about the time dependent fatigue characteristics of the stem cement interface is known. Thus, it was assumed a priori that complete debonding would occur, without consideration of the time frame.

Debonding was analyzed assuming 1 loading case, representing the stance phase of gait. However, other loading modes, such as stair climbing, may have considerable effects on the stress levels at the stem cement interface.[9] These authors found a 2 to 3-fold increase of peak stress at the interface under stair climbing loading conditions as compared with those of gait. Although these more severe loading conditions occur in much lower frequencies in daily activities, their effects on the failure process of the stem cement interface may be substantial but were not included in this study. Thus, this study is conceptual in nature, and the conclusions must be limited to the generic trends of the mechanisms unraveled.

The results indicate that debonding starts simultaneously at the tip and in the proximal medial region. Jasty et al[17] examined 16 retrieved femora and found stem cement debonding in all specimens. Locations where debonding most frequently occurred were the proximal anterior side and the tip region. This confirms the results found in the current analy-

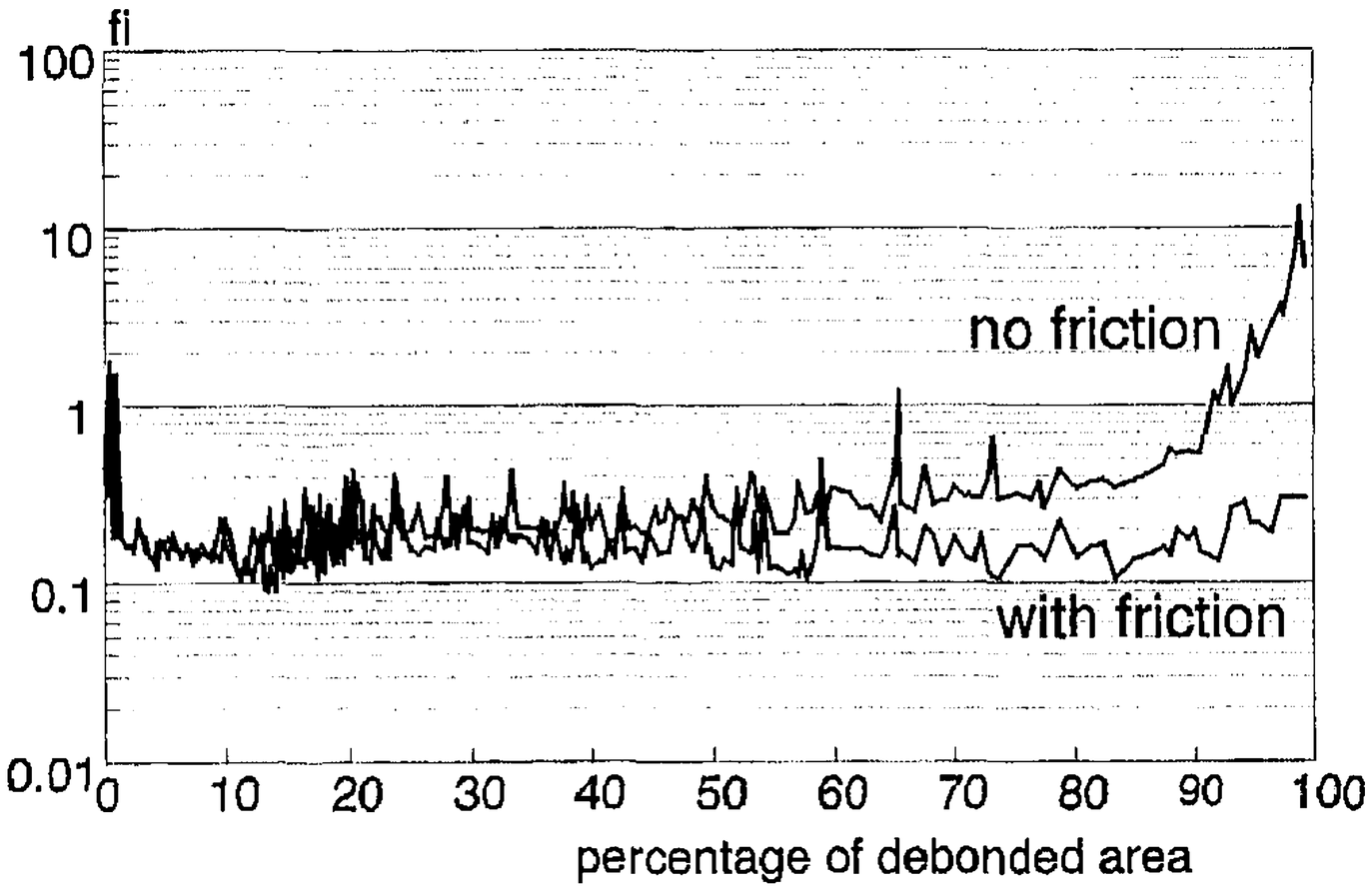

Fig 8. The development of the maximal failure index of the stem cement interface during the debonding process. After a high value at the beginning, the value remained at a rather constant level. After more 75% of the interface area had debonded, the index gradually increased. Assuming frictionless stem cement interface conditions at the debonded sites, resulted in higher cement stresses during the last part of the debonding process.

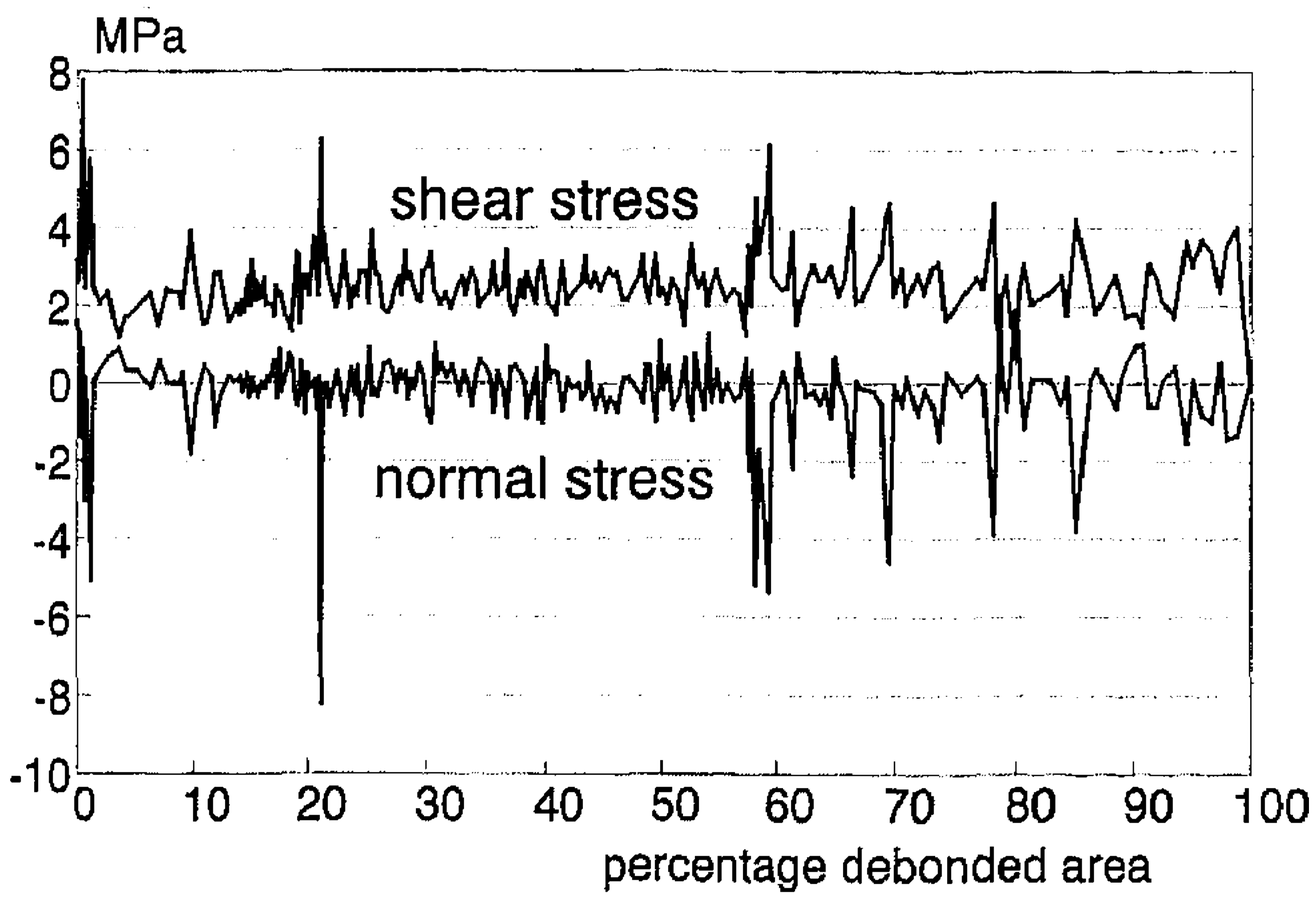

Fig 9. The contribution of the stress components (normal and shear) to the maximal failure index during the debonding process. During the whole debonding process, compressive and tensile stresses were much smaller than their static strengths, whereas the shear stress component reached values close to 6 MPa, which was assumed to be the static shear strength of the interface.

sis. Harrigan and Harris,[9] who studied the effects of partial stem cement debonding in a 3-dimensional finite element model, presumed that the tip of the distal stem was the last region to debond. This is not in accordance with the authors' results or those of Jasty et al.[17]

Around the edges of the debonded areas, high shear stresses at the stem cement interface were apparent where bonding remained. Consequently, this stress component governed the debonding process. This finding may be used to optimize the stem cement bonding characteristics. Increasing the shear strength seems more effective than improving the tensile strength of the interface. The important effect of the shear stress component on the debonding process also indicates that the results of the study performed by Lu et al[19] should be handled with great care. In that study, the authors neglected the shear stress at the stem cement interface and assumed that debonding was induced only by tensile stresses at the interface. With regard to the current study, such assumptions must be considered an oversimplification that may lead to unrealistic conclusions.

As debonding of the stem cement interface progressed, local stress peaks in the cement were generated at the edges of the bonded regions. This mechanism will promote local cement failure and may be the explanation of the occurrence of small cracks generated around partly loosened femoral components, as found by Jasty et al.[17] Despite these local stress peaks, the maximal stress peaks in the cement remained virtually unaffected until more than 50% of the interface area had debonded. After complete debonding, tensile peak stresses increased by a factor of 2, as compared with the case with a fully bonded interface. This is in accordance with data reported in the literature. Mann et al,[20] using finite element techniques and a stem cement friction coefficient of 0.22, found a stress increase of 2 to 3 times. Crowninshield and Tolbert[6] measured a 2-fold increase of proximal circumferential tensile stresses with an unbonded hip stem. Assuming no friction at the stem cement interface, the maximal tensile stress in the cement mantle increased by a factor of 6 after complete debonding. This finding is similar to those reported earlier in the literature. Assuming no friction at the interface, Harrigan and Harris[9] found stress levels that were 4.6 times higher, and Huiskes,[16] based on beam on elastic foundation theories, predicted a 4-fold increase of cement stresses.

Assuming that debonding occurs, it probably is a stable process, as shown in this study. During the major part of the debonding process, the value of the failure index remained at a constant level, well below 1. This indicates that debonding is not an immediate event but a fatigue process. Thus, it can be

expected that the debonding process will take a considerable amount of time before the interface is completely loose. This also can be deduced from the retrieval study of Jasty et al,[17] who found completely debonded interfaces in only 2 of the 16 specimens; the interfaces in the other specimens were only partly debonded. Simulating the stem cement debonding process, Lu et al[19] also found that partial debonding did not lead to increased interface stresses. Thus, stem cement debonding is a stable process. In other words, relative to the load applied, the bonded area of a full stem is overdimensioned. If the stem is fully bonded, interface stress concentrations occur distally and proximal medially. After debonding occurs here, the maximally stressed areas are rearranged, but the stresses do not increase. This implies that, mechanically speaking, a partially bonded stem is not less safe than a fully bonded one. This information could be used in designing stems with strategically placed coating patches or roughness patterns. These stems could be polished at locations where high postdebonding interface sliding is expected and roughened or coated where this is not the case to enhance partial bonding from the beginning.

References

1. Arroyo NA, Stark CF: The effect of textures, surface finish and precoating on the strength of bone cement/stem interfaces. Proceedings 13th Society for Biomaterials, New York 218, 1987.
2. Barb W, Park JB, Kenner GH, Recum AF: Intramedullary fixation of artificial hip joints with bone cement-precoated implants: I. Interfacial strengths. J Biomed Mater Res 16:447–458, 1982.
3. Bergmann G, Graichen F, Rohlmann A: Hip joint loading during walking and running, measured in two patients. J Biomech 26:969–990, 1993.
4. Carter DR, Hayes WC: The behavior of bone as a two-phase porous structure. J Bone Joint Surg 59A:954–962, 1977.
5. Crowninshield RD, Brand RA: A physiologically based criterion of muscle force prediction in locomotion. J Biomech 14:793–801, 1981.
6. Crowninshield RD, Tolbert JR: Cement strain measurement surrounding loose and well-fixed femoral component stems. J Biomed Mater Res 17:819–828, 1983.
7. Davies JP, O'Connor DO, Harris WH: Fatigue strength of cement/metal interfaces: Comparison of porous, precoated and smooth specimens. Proceedings 34th Orthopaedic Research Society, Atlanta 367, 1988.
8. Dostal WF, Andrews JG: A three-dimensional biomechanical model of hip musculature. J Biomech 17:803–812, 1981.
9. Harrigan TP, Harris WH: A three-dimensional nonlinear finite element study of the effect of cement-prosthesis debonding in cemented femoral total hip components. J Biomech 24:1047–1058, 1991.
10. Harrigan TP, Kareh JA, O'Connor DO, Burke DW, Harris WH: A finite element study of the initiation of fixation in cemented femoral total hip components. J Orthop Res 10:134–144, 1992.
11. Harris WH: Is it advantageous to strengthen the cement-metal interface and use a collar for cemented femoral components of total hip replacement? Clin Orthop 285:67–72, 1992.
12. Hoffman O: The brittle strength of orthotropic materials. J Comp Mat 1:200–206, 1967.
13. Huiskes R: Comparative stress patterns in cemented total hip arthroplasty. Orthop Rel Sci 1:93–108, 1990.
14. Huiskes R: Failed innovation in total hip replacement. Acta Orthop Scand 64:239–247, 1993.
15. Huiskes R: Mechanical failure in total hip arthroplasty with cement. Curr Orthop 7:239–247, 1993.
16. Huiskes R: Some fundamental aspects of human joint replacement. Acta Orthop Scand Suppl 185, 1980.
17. Jasty M, Maloney WJ, Bragdon CR, et al: The initiation of failure in cemented femoral components of hip arthroplasties. J Bone Joint Surg 73B:551–558, 1991.
18. Keller JC, Lautenschlager EP, Marshall GW, Meyer PR: Factors affecting surgical alloy/bone cement interface adhesion. J Biomed Mater Res 14:639–1651, 1980.
19. Lu Z, Ebramzadeh E, Sarmiento A: The effect of failure of the cement interfaces on gross loosening of cemented total hip femoral components. Proceedings 39th Orthopaedic Research Society, San Francisco 519, 1993.
20. Mann KA, Bartel DL, Wright TM, Burstein AH: Coulomb frictional interfaces in modeling cemented total hip replacements: A more realistic model. J Biomech 28:1067–1078, 1995.
21. Mann KA, Bartel DL, Wright TM, Ingraffea AR: Mechanical characteristics of the stem cement interface. J Orthop Res 9:798–808, 1991.
22. Raab S, Ahmed A, Provan JW: The quasistatic and fatigue performance of the implant/bone interface. J Biomed Mater Res 15:159–182, 1981.
23. Rohlmann A, Mossner U, Bergmann G, Kölbel R: Finite element analysis and experimental investigation in a femur with hip endoprosthesis. J Biomech 16:727–742, 1983.
24. Saha S, Pal S: Mechanical properties of bone cement: A review. J Biomed Mater Res 18:435–462, 1984.
25. Stone JL, Beaupre GS, Hayes WC: Multiaxial strength characteristics of trabecular bone. J Biomech 16:743–752, 1983.
26. Stone MH, Wilkinson R, Stother IG: Some factors affecting the strength of the cement-metal interface. J Bone Joint Surg 71B:217–221, 1989.

27. Verdonschot N, Huiskes R: Mechanical effects of stem cement interface characteristics in total hip replacement. Clin Orthop 329: 326–336,1996.

28. Weinans H, Huiskes R, Grootenboer HJ: Quantitative analysis of bone reactions to relative motions at implant-bone interface. J Biomech 11:1271–1282, 1993.